J. Mol. Model. **1997**, *3*, 216 – 223

A Molecular Model of CD86 and Analysis of Mutations which Disrupt Receptor Binding

Jürgen Bajorath

Bristol-Myers Squibb Pharmaceutical Research Institute, 3005 First Avenue, Seattle, WA 98121, Tel: (206) 727-3612, Fax: (206) 727-3602 (bajorath@protos.bms.com) and Department of Biological Structure, University of Washington, Seattle, WA 98195.

Received: 27 March 1997 / Accepted: 12 May 1997 / Published: 20 May 1997

Abstract

CD86 and its homologue CD80 are type I transmembrane proteins expressed on antigen presenting cells. CD80 and CD86 specifically interact with CD28 and CD152 on T cells. This interaction results in T cell costimulation and complements T cell receptor signaling. The extracellular regions of CD80 and CD86 contain two immunoglobulin-like domains. In the presence of low sequence similarity to proteins with known three-dimensional structure, a molecular model of the N-terminal receptor-binding domain of human CD86 was built based on consensus residue analysis and structure-oriented sequence comparison. The model was assessed by energy profile analysis and regions of high, medium, and low prediction confidence were identified. Several CD86 point mutations which abolish receptor binding map to high confidence regions of the model. This has made it possible to rationalize their effects on binding or structure.

Key words: Sequence-structure comparison, key residues, immunoglobulin fold, protein modeling, model analysis

Introduction

Interactions between cell surface proteins CD80/CD86 on antigen presenting cells and CD28/CD152 on T cells complement T cell receptor signaling [1]. These ligand-receptor interactions trigger costimulatory signals which are required for effective T cell proliferation and activation [1]. Both CD80/CD86 and CD28/CD152 belong to the immunoglobulin superfamily (IgSF) [2]. While CD28 and CD152 each contain a single extracellular immunoglobulin (Ig) domain, both CD80 and CD86 contain two extracellular Ig domains [3]. The stoichiometry of the CD80/CD86-CD28/CD152 interactions is 1:1 [3,4]. Numerous mutagenesis experiments on CD80 have been reported [5,6]. Although mutations of residues in both domains of CD80 compromise, directly or indirectly, the interaction with CD28/CD152 [5,6], the N-terminal domain was shown to be sufficient for ligand binding [6,7]. Based on sequence comparisons and approximate mapping on Ig folds, many residues in the N-terminal domain of CD80 which are, on the basis of mutagenesis, important for receptor binding, map to one β–sheet of the domain [5,6].

An important feature of CD80 and CD86 is their limited sequence conservation. Despite common receptor binding properties and similar functions, these proteins share only ~30% sequence conservation in their extracellular region [8]. This level does not much exceed sequence similarities of ~15-20% observed for many IgSF proteins with unrelated func-

Correspondence to J. Bajorath, BMS-PRI, 3005 First Avenue, Seattle, WA 98121

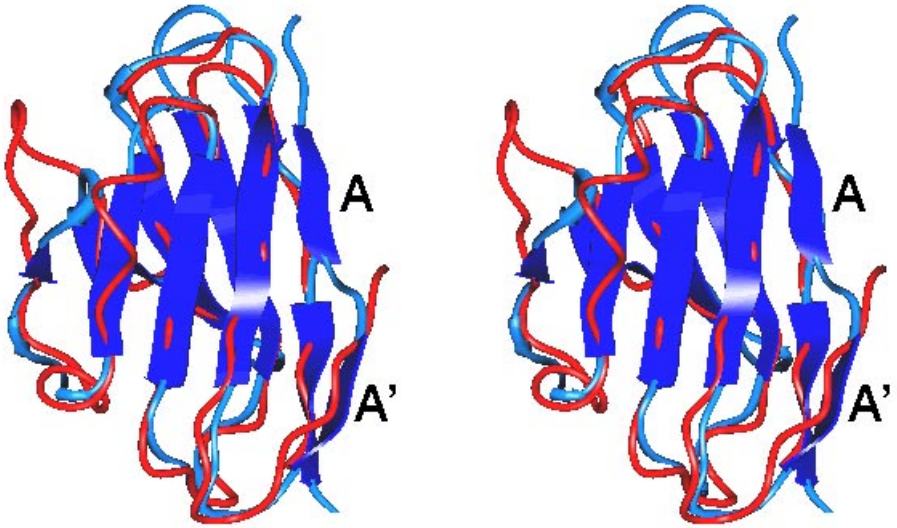

Figure 1a. *Structure-based sequence analysis. Superposition of the VL domain of REI (blue) and the V-domain of CD4 (red) is shown. The β-strands in REI are shown as dark blue bands. The A- and A'-strands are labeled. The stereo view focuses on the β-sheet surface formed by strands (from the right to the left) A-B-E-D. The A'-strand belongs to the opposite (A'-G-F-C-C'-C") β-sheet. CD4 does not include an A-strand. In this orientation, the antibody Complementarity Determining Region (CDR) loops (B-C, C'-C", F-G) are at the top.*

tions [2]. The majority of Ig domains are either V(ariable)- or C(constant)-type structures [2]. The sequences of the N-terminal CD80/CD86 domains are more similar to V-domains than other IgSF structure types, while the second domains display C-type characteristics [8,9]. Threading calculations using the topological fingerprint technique [10] suggested significant sequence-structure compatibility of the CD80/CD86 second domains with Ig C-type folds, but failed to identify clear similarities between the N-terminal domains and available three-dimensional (3D) structures [11]. No 3D models are currently available for the receptor binding domain of CD80 or CD86.

CD86 was identified later than CD80 [9] and is less well studied. Limited mutagenesis data on the N-terminal domain of CD86 is available [6] but has not been analyzed in detail. Thus, a molecular model would be helpful to provide some insights into the structure and binding characteristics of CD86. Here it was attempted to model the N-terminal extracellular domain of human CD86. The approach was similar to a previous protocol used to build a 3D model of CD152 [12]. IgSF consensus residue based sequence analysis and structure comparison [13-15] were used in combination with comparative modeling methods [15,16]. High confidence regions of the model were identified. These regions include several residues which, when mutated, disrupt CD28/CD152 binding. These residues were mapped and effects resulting from their mutation predicted.

Methods

Sequence searches were performed using GCG programs (Genetics Computer Group, Madison, WI). An alignment of human and mouse CD80/CD86 sequences [8] was combined with a topological sequence alignment of representative IgSF V-set [2] structures including the antibody variable light (VL) chain of REI [17], the variable heavy (VH) chain of KOL [18], and the V-like domains of CD2 [19], CD4 [20], and CD8 [21]. The topological alignment was based on pairwise alpha carbon superposition of these structures, which were performed using ALIGN [22]. Due to low sequence similarities, CD80/CD86 sequences were incorporated manually by aligning IgSF V-set consensus residues [2,14].

Model building of CD86 was based on the first domain of CD4 (pdb code "3cd4") as structural template. Modeling and structural manipulations were carried out using InsightII (MSI, San Diego, CA). Color images were produced with InsightII and processed as Silicon Graphics RGB files. The side chains of conserved residues were copied to the model and conservative residue replacements in core regions were carried out in conformations as similar as possible to the original side chain. Other side chains were modeled in groups of spatially adjacent residues using a low energy rotamer search technique [23].

Two loop conformations (C"-D, E-F) were modeled based on the corresponding loops in CD4 and β–turns were built interactively. Other loop conformations were modeled by systematic conformational search using CONGEN [24]. For the long B-C and F-G loops, possible conformations were generated by partial conformational search. In each case, CONGEN-generated loop conformations with negative potential energy were sampled, and the conformation with smallest solvent-accessible surface within 3 kcal/mol (1 kcal = 4.18 kJ) of the energy minimum conformation was included in the model. Side chain conformations of residues in CONGEN-modeled loops were adjusted to similar rotamer conformations using InsightII.

The stereochemistry and intramolecular contacts of the model were refined by conjugate gradients energy minimization with Discover (MSI, San Diego, CA) using AMBER force field parameters [25], a distance-dependent dielectric constant (1r), and a 10 Å cutoff distance for non-bonded in-

```
            ___A___   __A′__      ____B____             ___C___
              *         *         * * *                 * *
REI    VL: DIQMTQS PSSLSAS VGD RVTITCQAS QDIIK----- YLNWYQQ TPGKA--
KOL    VH: EVQLVQS GG-GVVQ PGR SLRLSCSSS GFIFSSY--- AMYWVRQ APGKG--
CD8    V : -SQFRVS PLDRTWN LGE TVELKCQVL LSNPTS---- GCSWLFQ PRGAAAS
CD4    D1: ------- KKVVLGK KGD TVELTCTAS QKKSI----- QFHWKN- SN-----
CD2    D1: ------- SGTVWGA LGH GINLNIPNF QMTDDID--- EVRWER- GS-----
hCD86  D1: ------- -IQAYF- NE- TADLPCQFA NSQNQSLSEL VVFWQD- QE-----
mCD86  D1: ------- -TQAYF- NG- TAYLPCPFT KAQNISLSEL VVFWQD- QQ-----
hCD80  D1: ------- -VTKEV- KE- VATLSCGH- NVSVEELAQT RIYWQK- EK-----
mCD80  D1: ------- -LSKSV- KD- KVLVPCRY- NSPHEDESED RIYWQK- HD-----
                   5                   20         30

            ___C′___        _C″_          __D___        ___E____
              **            **              * * *   *   *
REI    VL: PKLLIYE- AS--- NLQA GVPS--- RFSGSG SG--- TDYTFTIS SLQPEDI
KOL    VH: PEWVAIIW DDGSD QHYA DSVKG-- RFTISR NDSK- NTLFLQMD SLRPEDT
CD8    V : PTFLLYLS QNKP- KAAE GLDTQ-- RFSGKR LG--- DTFVLTLS DFRRENE
CD4    D1: QIKILGNQ GS--- FLTK GPSKLND RADSRR SLWDQ GNFPLIIK NLKIEDS
CD2    D1: -TLVAEFK RKMK- PFLK SG----- AFEIL- A---- -NGDLKIK NLTRDDS
hCD86  D1: -NLVLNEV YLGKE KFDS VHSKYMG RTSFD- SD--- -SWTLRLH NLQIKDK
mCD86  D1: -KLVLYEH YLGTE KLDS VNAKYLG RTSFD- RN--- -NWTLRLH NVQIKDM
hCD80  D1: -KMVLTMM S---- GDMN IWPEYKN RTIFD- ITN-- -NLSIVIL ALRPSDE
mCD80  D1: -KVVLSVI A---- GKLK VWPEYKN RTLYD- NT--- -TYSLIIL GLVLSDR
             40               55                     70

            ___F___                  _____G_____
              * *                        * *
REI    VL: ATYYCQQ YQSLP---------- YTFGQGTKLQIT
KOL    VH: GVYFCAR DGGHGFCSSASCFGP DYWGQGTPVTVS
CD8    V : GYYFCSA LSNSI---------- MYFSHFVPVFLP
CD4    D1: DTYICE- VE------------- -DQKEEVQLLVF
CD2    D1: GTYNVTV YSTNGTR-------- -ILDKALDLRIL
hCD86  D1: GLYQCII HHKKPTGMI------ RIHQMNSILSVL
mCD86  D1: GSYDCFI QKKPPTGSI------ ILQQTLTELSVI
hCD80  D1: GTYECVV LKYEKDAFK------ REHLAEVTLSVK
mCD80  D1: GTYSCVV QKKERGTYE------ VKHLALVKLSIK
             85                            110
```

Figure 1b. *Structure-based sequence analysis. Alignment of CD80/CD86 V-domain sequences (h: human, m: mouse) with representative X-ray structures (REI, KOL, CD8, CD4, CD2; VL: variable light, VH: variable heavy, D1: V-like extracellular domain 1). Average strand assignments are shown. CD80/CD86 sequences were included in the alignment by matching conserved core positions (labeled with asterisks). Most of these positions are IgSF V-set consensus residues. Sequence numbers are given for human CD86.*

teractions. Minimization was carried out until the maximum derivative of the energy function was approximately 20 kcal/mol. At this stage, no unfavorable contacts were detected in the model and no non-glycine residues were found in disallowed torsional space. In addition, backbone hydrogen bonding interactions between β–strands were conserved. Contact and stereochemical analyses were performed with Procheck [26]. The sequence-structure compatibility of the model was analyzed and compared to CD4 using the energy profile method [27] as implemented in the Prosa 4.0 program, which was generously provided by M. Sippl and H. Flöckner, University of Salzburg. Protein backbone atoms were used to calculate the profiles, and a 10 residue window was used for energy averaging at each position.

Results and Discussion

CD80 and CD86 do not show significant similarities to sequences of proteins with known 3D structure available in the Brookhaven Protein Data Bank [28]. With the exception of antibodies, the low level of sequence conservation between IgSF proteins [2] makes the application of comparative modeling techniques difficult [16]. Therefore, structure-based sequence analysis was a focal point in the modeling of CD86.

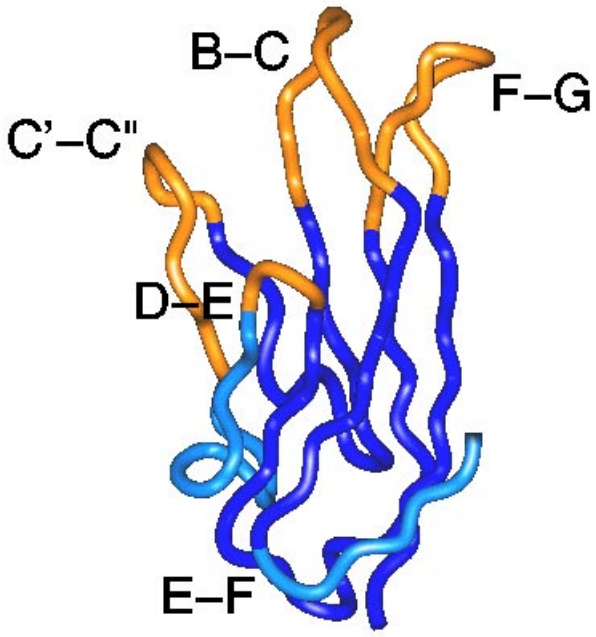

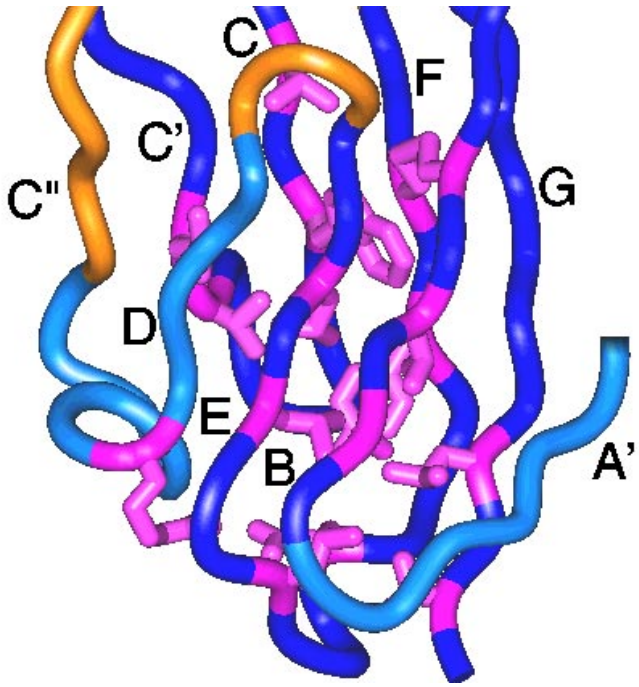

Figure 2a. *Schematic representation of the CD86 molecular model is shown with regions color-coded according to expected prediction accuracy (see text). Regions of high prediction confidence are colored dark blue and medium confidence regions are colored light blue. Regions with low prediction confidence, which can not be discussed beyond the level of a schematic view, are colored yellow. Selected loops are labeled.*

Figure 2b. *The CD86 molecular model. A close-up view is shown including the IgSF consensus residues (magenta) which were used as anchor points for the sequence alignment. Selected β-strands are labeled.*

The Ig fold is formed by two tightly packed curved β–sheets, each consisting of four to six β–strands [14,15]. The sheets are connected by loops following conserved topology. Different Ig variants or folding types have been classified based on the number and spatial arrangement of β-strands [2,13,14]. The two β-sheets of the V-fold typically consist of four (A-B-E-D) and six (A'-G-F-C-C'-C") strands, respectively, with the A strand split between the two sheets (A/A'). Loop sizes and conformations and the arrangements of β–strands at the edges of the sheets may vary greatly even in structures of the same IgSF type. This is illustrated in Figure 1a which shows a superposition of two Ig V-type structures, the first domain of CD4 and the VL domain of REI. The sequences of representative Ig V-like structures were aligned based on superpositions (Figure 1b). The alignment reflects spatial equivalence of residues in β–strands and some conserved loops (A'-B, E-F). Structurally conserved IgSF positions are discussed below.

Sequence conservation among many IgSF proteins is often reduced to a set of conserved consensus/key residues which determine the Ig fold. Overlapping but distinct sets of consensus residues characterize different IgSF structure types [2,13,14]. Many IgSF consensus residues are hydrophobic, participate in the formation of the core, and superpose well when different IgSF structures are compared. For example, the B-, C-, E-, and F-strands display highly conserved patterns of consensus residues, while consensus residues are absent in other regions, for example, the C"-strand. Conserved or conservatively replaced residues in CD80/CD86 were identified and, if possible, matched to IgSF consensus positions. The final alignment is shown in Figure 1b. As noted previously [6,11], the sequences of the CD80/CD86 family display some IgSF signature residues [2,14,15]. These residues include two cysteines, separated by 60-70 residues, and a highly conserved tryptophane approximately 15 residues following the first cysteine. The conserved Ig cysteines are part of β–strands B and F, and the tryptophane belongs to the C-strand. There is no stringent requirement for the conservation of all consensus residues in IgSF V-type structures. For example, the canonical disulfide bond is absent in CD2 [19].

CD80/CD86 sequence segments corresponding to β–strands B, C, E, and F include the characteristic IgSF sequence patterns, which makes the strand assignments unambiguous. Hydrophobic IgSF consensus residues could also be assigned to the C'- and G-strands. The D-strand only includes the conserved arginine at the beginning, which forms a salt bridge to an aspartic acid in the E-F loop. This is the most conserved loop in Ig V-domains and its signature sequence motif is also present in CD80/CD86. Approximately 30 residues separate the predicted C- and E-strands in the

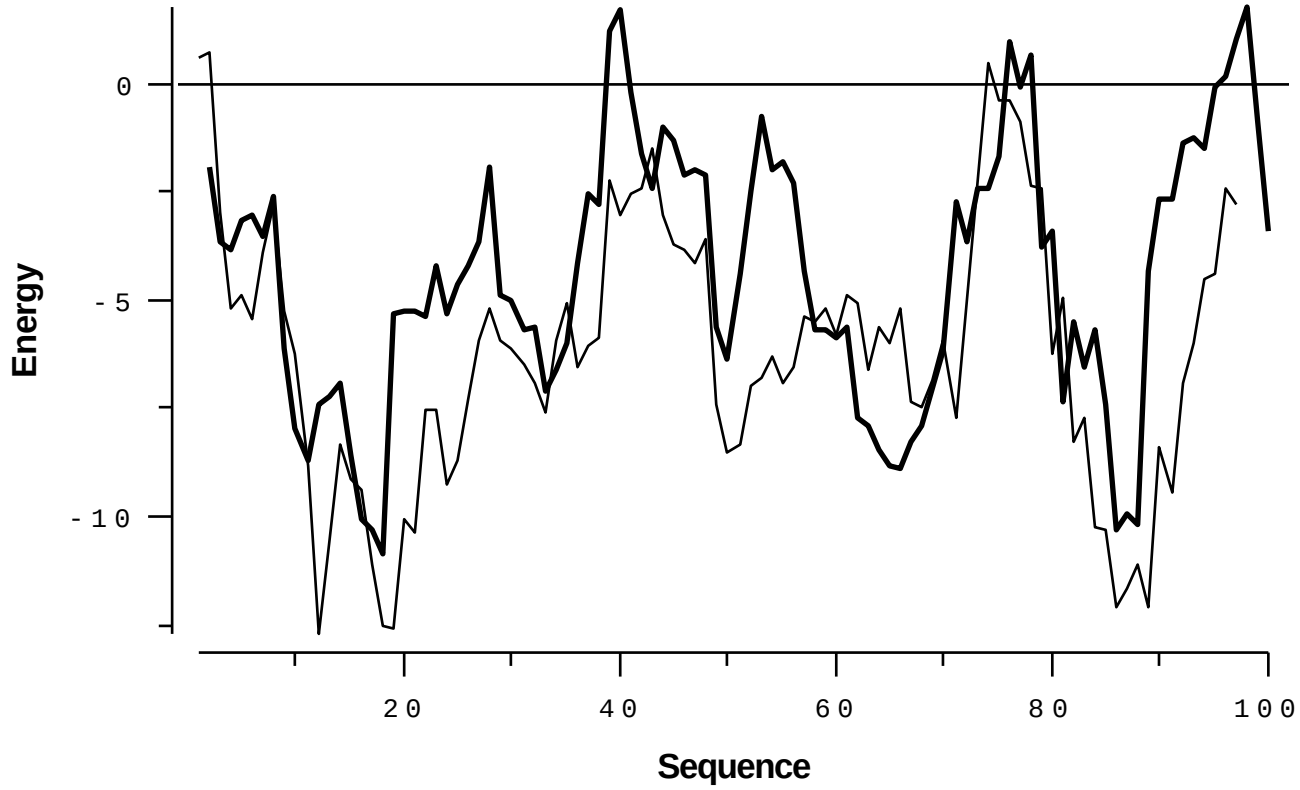

Figure 2c. *Energy profile of the CD86 model (thick line) compared to CD4 D1 (thin line). The profiles were calculated using a 10 residue window for energy averaging. Residue interaction energy is given in E/kT (E, interaction energy in kcal/mol (1 kcal = 4.18 kJ); k: Boltzmann constant; T: absolute temperature in Kelvin).*

CD80 and CD86, which is a characteristic feature of IgSF V-type structures [14].

Two regions could not be assigned with confidence. The C"-strand at the edge of the β–sheet and the C'-C" loop do not include IgSF consensus residues. In addition, residues approximately corresponding to this region were not conserved in CD80/CD86. Thus, no meaningful sequence to structure alignment was possible for the C'-C" loop and the C"-strand. In addition, the assignment of the N-terminal A/A'-strands was difficult. The A/A'–strand switch from one β–sheet to the other is marked by the presence of a conserved proline or, in some cases, glycine residue. V-domains which lack these signature residues such as CD2 or CD4 usually do not include the A-strand. Similar to the C"-region, the N-terminal sequences of CD80/CD86 were not conserved and did not include A-strand or strand switch consensus residues. Therefore, the absence of the A-strand was predicted.

Human CD86 was modeled based on the sequence to structure alignment in Figure 1b. Sequence similarities between all compared structures and CD80/CD86 were low. Considering the predicted absence of the A-strand, CD4 was selected as the template for model building. The identity between CD4 and CD86 sequences in the modeled region is only ~13%, which emphasizes the critical role of consensus residues as anchor points for the alignment. The backbones of the core β–strands were copied to the model prior to the modeling of side chain and loop conformations. A shortened A'-strand and a tentative C"-strand were included in the model. The highly conserved E-F loop and the C"-D loop were modeled based on CD4. The model was refined by energy minimization, and the stereochemical quality of the model was confirmed.

Figure 2a shows an outline of the CD86 model. The B-C, C'-C", and F-G loops map to the same side of the domain. In antibodies, these (Complementarity Determining Regions) COR loops form the antigen binding site. In CD86, these loops or, alternatively, the adjacent β-strands are longer than in many other (non-antibody) IgSF proteins, and their conformations were thus more difficult to predict. Figure 2b shows the IgSF consensus resisues in the CD86 model. These residues participate in the formation of the hydrophobic core. The figure also shows that the A'- and C"-strands at the edges of the sheet lack structural stabilization. Despite low sequence identity with the compared structures, the majority of IgSF V-domain consensus residues could be identified in CD86 and confidently modeled. Energy profile analysis was used to more quantitatively assess the sequence-structure compatibility of the model (**Figure 2c**). The residue interaction en-

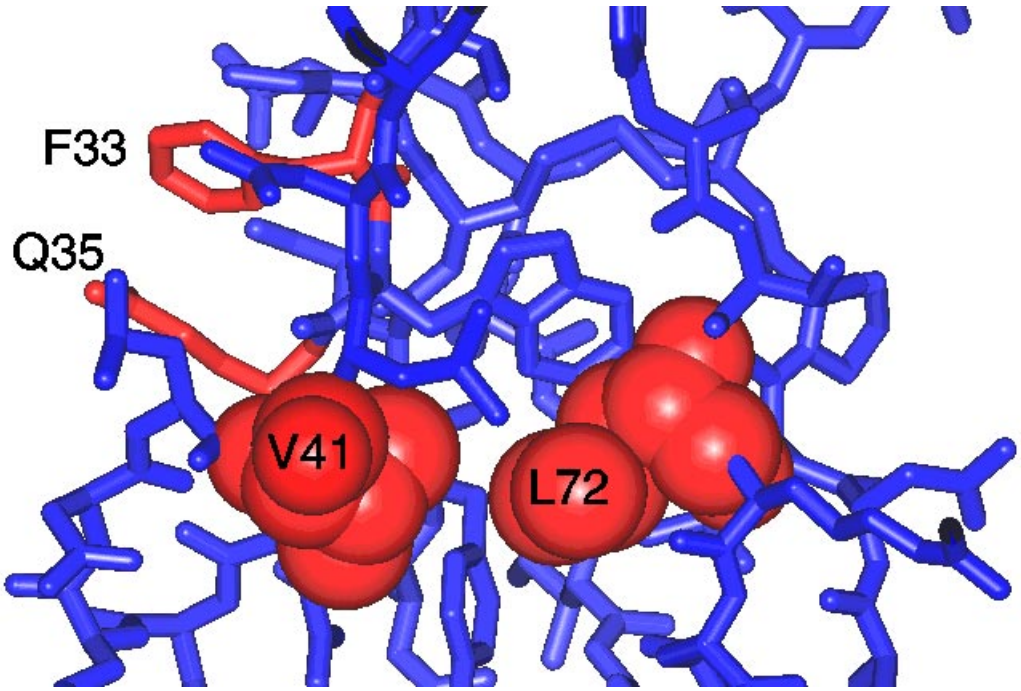

Figure 3a. *Mapping of CD86 mutants. Residues whose mutation to alanine disrupts CD28 and CD152 binding are shown in red and are labeled. A side view of the high confidence regions is shown. The G-F-C-C' b-sheet surface is on the left. Both V41 and L72 are buried in the core regions.*

ergy profiles for CD86 model and the CD4 structure were found to be overall similar in shape and average energies. Although these profiles are not sensitive to incorrectly modeled side chain and many loop conformations, the absence of significant errors in the core regions of the CD86 model was suggested. These findings were consistent with the conclusions drawn from the alignment of consensus residues.

In order to discuss details of the CD86 model beyond the level of an outline structure, regions were classified according to expected prediction accuracy. Regions of high prediction confidence include β–strands with unambiguous periodicity (e. g., B), as defined by the presence of several IgSF consensus residues. High confidence regions also include conserved loops (E-F) and short turns between well-defined strands (e. g. C-C'). In high confidence regions, buried and surface residues, their spatial arrangement and should be correctly predicted. Structural elements were considered medium confidence regions if the identification of consensus residues was incomplete (D-strand) or difficult (A'-strand). The conformations of medium confidence regions were considered approximate but not suitable for analysis at the residue level of detail. Low confidence regions include long loops (e. g. B-C), whose conformations are difficult to predict by both ab initio [24] and database search [29] methods, and regions which lack IgSF consensus residues or other sequence similarities (e. g., C"). The conformations of low confidence regions were considered possible but tentative. Following these criteria, high confidence regions include β–strands B, C, C', E, F, G and the C-C' and E-F loops. Medium confidence regions include strands A' and D and the A'-B and C"-D loops, and low confidence regions include the C"-strand and loops B-C, C'-C", D-E, and F-G (Figure 2a).

The model was used to analyze the location and putative effects of previously reported CD86 point mutants. For a detailed analysis, only regions of high prediction confidence were considered. Mutation of five CD86 residues (F33, Q35, V41, Y59, L72) to alanine were found to abolish the binding to both CD28 and CD152 [6]. These residues belong to the limited number of residues in the N-terminal domain which are conserved in CD80 and CD86 across species. Four of these residues (except Y59) map to high confidence regions of the CD86 model. F33 and Q35 are part of the C-strand, while V41 and L72 belong to the C'- and E-strand, respectively. Figure 3a shows the predicted location of these residues. V41 and L72 map to IgSF core positions and their side chains are in contact distance in the model. Mutations of these residues are expected to compromise the integrity of the hydrophobic core. Thus, the loss of receptor binding is probably the result of structural perturbations. In contrast, both F33 and Q35 map to solvent-exposed positions on the G-F-C-C' β–sheet surface (Figure 3b). In these cases, mutations to alanine are not expected to perturb the 3D structure. Therefore, both residues are predicted to form critical contacts upon receptor binding. The location of these residues implies that the G-F-C-C' face of the domain is involved in binding to CD28/CD152, similar to what has been proposed

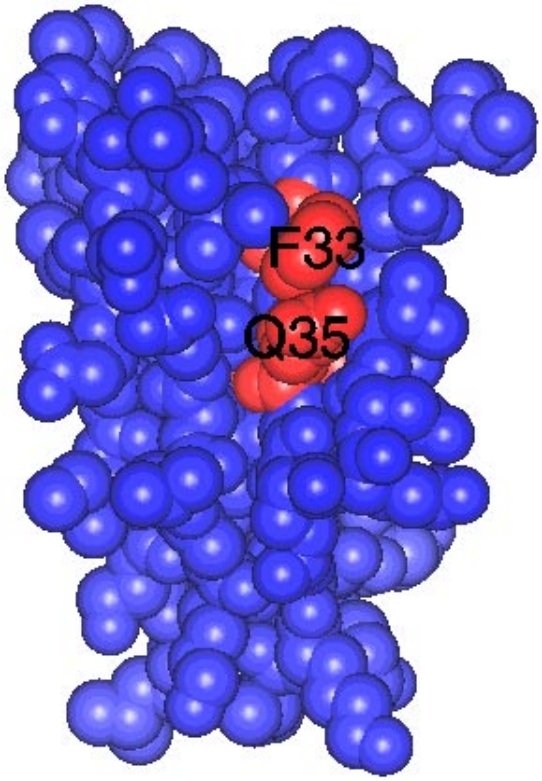

Figure 3b. *Mapping of CD86 mutants. The view is obtained by approximately 90 degree rotation around the vertical axis and focuses on the G-F-C-C' face. The space-filling representation illustrates that, in contrast to V41 and L72, both Q35 and F33 are accessible on the protein surface and available for receptor binding.*

for CD80 [6]. Since the corresponding β–sheet surface of the ligand binding domain of CD152 contains residues implicated in CD80/CD86 binding [12], a face-to-face interaction between the N-terminal Ig domains may play a major role in the formation of CD80/CD86-CD28/CD152 ligand-receptor complexes.

Conclusions

A three-dimensional model of the N-terminal extracellular domain of human CD86 was constructed by comparative modeling. Due to low sequence conservation, model building was critically dependent on IgSF consensus residue analysis. The model, which was sound on the basis of stereochemical and energy profile analysis, was divided into regions of high, intermediate, and low prediction confidence. Four previously reported CD86 point mutations, which disrupt receptor binding, map to high confidence regions in the model and were analyzed. Two of the targeted residues occupy core positions, while two other residues are exposed on the G-F-C-C' β–sheet surface and available for receptor binding. The study presented herein provides a basis for modeling the 3D structures of other members of the CD80/CD86 family.

References

1. Linsley, P. S.; Ledbetter, J. A. *Ann. Rev. Immunol.* **1993**, *11*, 191.
2. Williams, A. F.; Barclay, A. N. *Ann. Rev. Immunol.* **1988**, *6*, 381.
3. Linsley, P. S.; Ledbetter, J.; Peach, R.; Bajorath, J. *Res. Immunol.* **1995**, *146*, 130.
4. Linsley, P. S.; Nadler, S. G.; Bajorath, J.; Peach, R. J.; Leung, H.; Rogers, J.; Bradshaw, J.; Stebbins, M.; Leytze, G.; Brady, W.; Malacko, A. R.; Marquardt, H.; Shaw, S.-Y. *J. Biol. Chem.* **1995**, *270*, 15417.
5. Fargeas, C.A.; Truneh, A.; Reddy, M.; Hurle, M.; Sweet, R.; Sekaly, R.-P. *J. Exp. Med.* **1995**, *182*, 667.
6. Peach, R. J.; Bajorath, J.; Naemura, J.; Leytze, G.; Greene, J., Aruffo, A.; Linsley, P. S. *J. Biol. Chem.* **1995**, *270*, 21181.
7. Inobe, M.; Linsley, P. S.; Ledbetter, J. A.; Nagai, Y.; Tamakoshi, M.; Uede, T. *Biochem. Biophys. Res. Commun.* **1994**, *200*, 443.
8. Linsley, P. S.; Peach, R. J.; Gladstone, P.; Bajorath, J. *Protein Science* **1994**, *3*, 1341.
9. Freeman, G. J.; Gribben, J. G.; Boussiotis, V. A.; Ng, J. Y.; Restivo, V. A., Jr.; Lombard, L. A.; Gray, G. S.; Nadler, L. M. *Science* **1993**, *262*, 909.
10. Godzik, A.; Kolinski, A.; Skolnick, J. *J. Mol. Biol.* **1992**, *227*, 227.
11. Bajorath, J.; Peach, R. J.; Linsley, P. S. *Protein Science* **1994**, *3*, 2148.
12. Bajorath, J.; Linsley, P. S. *J. Mol. Model.* **1997**, *3*, 117.
13. Harpaz, Y.; Chothia, C. *J. Mol. Biol.* **1994**, *238*, 528.
14. Bork, P.; Holm, L.; Sander, C. *J. Mol. Biol.* **1994**, *242*, 309.
15. Novotny, J.; Bajorath, J. *Adv. Prot. Chem.* **1996**, *49*, 149.
16. Bajorath, J.; Stenkamp, R.; Aruffo, A. *Protein Science* **1993**, *2*, 1798.
17. Epp, O.; Lattman, E. E.; Schiffer, M.; Huber, R.; Palm, W. *Biochemistry* **1975**, *14*, 4943.
18. Marquardt, M.; Deisenhofer, J.; Huber, R.; Palm, W. *J. Mol. Biol.* **1980**, *141*, 369.
19. Jones, E. Y.; Davis, S. J.; Williams, A. F.; Harlos, K.; Stuart, D. I. *Nature* **1992**, *360*, 232.
20. Ryu, S.-E.; Kwong, P. D.; Truneh, A.; Porter, T. G.; Arthos, J.; Rosenberg, M.; Dai, X.; Xuong, N.-H.; Axel, R.; Sweet, R. W.; Hendrickson, W. A. *Nature* **1990**, *348*, 419.
21. Leahy. D. J.; Axel, R.; Hendrickson, W. A. *Cell* **1992**, *68*, 1145.
22. Satow, Y.; Cohen, G. H.; Padlan, E. A.; Davies, D. R. *J. Mol. Biol.* **1986**, *190*, 593.

23. Bajorath, J.; Fine, R. M. *Immunomethods* **1992**, *1*, 137.
24. Bruccoleri, R. E.; Novotny, J. *Immunomethods* **1992**, *1*, 96.
25. Weiner, S. J.; Kollman, P. A.; Nguyen, D. T.; Case, D. A. *J. Comp. Chem.* **1986**, *7*, 230.
26. Laskowski, R. A.; MacArthur, M. W.; Moss, D. S.; Thornton, J. M. *J. Appl. Cryst.* **1993**, *26*, 283.
27. Sippl, M. J. *Proteins: Structure, Function, and Genetics* **1993**, *17*, 355.
28. Bernstein, F. C.; Koetzle, T. F.; Williams, G. J. B.; Meyer, E. F., Jr.; Brice, M. D.; Rodgers, J. R.; Kennard, O.; Shimanouchi, T.; Tasumi, M. *J. Mol. Biol.* **1977**, *112*, 535.
29. Jones, T. A.; Thirup, S. *EMBO J.* **1986**, *5*, 819.